A new parameterization method for Dissipative Particle Dynamics

Karl P. Travis[*1], Mark Bankhead[2], Kevin Good[1], and Scott L. Owens[2]

[1]*Immobilisation Science Laboratory, Department of Engineering Materials, University of Sheffield, Mappin Street, Sheffield S1 3JD, UK.*

[2]*Nexia Solutions Ltd., Hinton House, Warrington, Cheshire, WA3 6AS, UK.*

* Corresponding author (Email k.travis@sheffield.ac.uk)

ABSTRACT

We introduce an improved method of parameterizing the Groot-Warren version of Dissipative Particle Dynamics (DPD) by exploiting a correspondence between DPD and Scatchard-Hildebrand regular solution theory. The new parameterization scheme widens the realm of applicability of DPD by first removing the restriction of equal repulsive interactions between like beads, and second, by relating *all* conservative interactions between beads directly to cohesive energy densities.

We establish the correspondence by deriving an expression for the Helmoltz free energy of mixing obtaining a heat of mixing which is exactly the same form as that for a regular mixture (quadratic in the volume fraction) and an entropy of mixing which reduces to the ideal entropy of mixing for equal molar volumes. We equate the conservative interaction parameters in the DPD force law to the cohesive energy densities of the pure fluids providing an alternative method of calculating the self-interaction parameters as well as a route to the cross-interaction parameter.

We validate the new parameterization by modelling the binary system: $SnI_4/SiCl_4$, which displays liquid-liquid coexistence below an upper critical solution temperature around 140˚C. A series of DPD simulations were conducted at a set of temperatures ranging from 0˚C to above the experimental upper critical solution temperature using conservative parameters based on extrapolated experimental data. These simulations can be regarded as being equivalent to a quench from a high temperature to a lower one at constant volume.

Our simulations recover the expected phase behaviour ranging from solid-liquid coexistence to liquid-liquid co-existence and eventually leading to a homogeneous single

phase system. The results yield a binodal curve in close agreement with one predicted using regular solution theory, but, significantly, in closer agreement with actual solubility measurements.

I. INTRODUCTION

Dissipative Particle Dynamics (DPD) is one of the most promising methods for modelling complex multi-phase materials developed in the last 20 years. It was developed in the early 1990s by Hoogerbrugge and Koelman [1] as a tool for simulating fluids from the mesoscale (10-100 nm and 10-100 ns) to the continuum limit. The method represents matter as a set of point particles, the distribution and density of which is determined by a set of prescribed forces. Each of these point particles represents a "bead" of fluid. The molecular structure of the fluid has been eliminated in the coarse grained description of matter. The method shares features of both Molecular Dynamics and Lattice Gas Automata and closely resembles the structure of a Brownian Dynamics algorithm, having stochastic, dissipative and conservative forces. The conservative forces act to distribute the beads in space as evenly as possible to minimise free energy. The dissipative force represents friction and acts to reduce velocity differences between the beads. The stochastic force represents the degrees of freedom that have been eliminated in the coarse graining of matter. The magnitude of the stochastic and dissipative forces is coupled by fluctuation-dissipation theorem and this acts as a system thermostat.

DPD has been improved several times since its introduction, most notably by Español and Warren [2], and then by Groot and Warren [3]. The advantages of DPD are that the algorithm retains a very simple structure, it recovers hydrodynamic behaviour, and can be used to study various types of fluid flow without the need for implicit solvents (which are modelled explicitly in DPD), is off-lattice, and, due to the pair-wise nature of

the conservative forces, can be extended to multi-component systems using a simple two-dimensional matrix of like-like and like-unlike terms.

A major weakness in the current application of DPD is that the method for deriving the key interaction parameters has been, since its introduction by Groot and Warren (GW), grounded in polymer science, through the application of Flory-Huggins (FH) theory. It has become common practise when simulating mixtures using DPD to treat AA type interactions as being no different to BB type interactions. Furthermore the strength of these like-like bead interactions is often related to the isothermal compressibility of ambient water. This choice of parameterization was merely suggested by GW, presumably as a consequence of the correspondence between DPD and FH theory. However, these suggestions have unjustifiably become inseparable from the algorithm; applications abound in which this parameterization is effectively used, including simulation of lipids [4] block copolymers [5], vesicle formation of amphiphilic molecules [6], surfactants [7] and graft fluorinated co-oligomers [8]. A rich range of phase behaviour has been observed in many of these simulations but in all cases, quantitative comparison with experiment is lacking; a DPD fluid will phase separate, but the compositions of the resulting coexisting phases are necessarily symmetric and often somewhat arbitrary. Clearly the phase compositions depend on the chemical details of the various components and this must be taken into account if DPD is to become a serious tool for modelling the phase behaviour of complex fluids.

In this paper we address the issue of parameterizing the DPD conservative forces. We first demonstrate that GW DPD has essentially the same form of the free energy of mixing as that in Scatchard-Hildebrand regular solution theory. Having established this

correspondence we then show how the entire conservative interaction matrix can be determined using the cohesive energy densities of the pure components of a binary mixture. We demonstrate that this method of parameterization is internally consistent by considering the phase equilibria in the binary system, Stannic(IV)iodide (SnI_4) / tetrachlorosilane ($SiCl_4$). The conservative force parameters for this system are obtained using experimental solubility and heat of vaporisation data [9]. Our DPD simulations are broadly in agreement with both experimental solubility data and with the predictions of regular solution theory; we observe solid-liquid and liquid-liquid coexistence, as well as a single homogeneous phase close to the experimental upper critical solution temperature (UCST). By contrast, we show that DPD simulations employing equal like-like bead interactions do not give rise to the expected phase behaviour.

II. THE DPD ALGORITHM

The original DPD method, first introduced by Hoogerbrugge and Koelman, has been modified over the years, most notably by Pagonabarraga and Frenkel, who introduced a density dependent conservative force into the algorithm [10]. We prefer the version of DPD as described in the paper by Groot and Warren (GW) based on its greater simplicity [3]. We shall henceforth refer to this as the GW DPD algorithm. Since GW DPD has been described in detail elsewhere we give only a brief summary of it here. A system of beads interact with each other as a result of pairwise additive forces comprising of conservative forces, $\boldsymbol{F}^C$, dissipative forces, $\boldsymbol{F}^D$, and a random forces, $\boldsymbol{F}^R$:

$$\boldsymbol{F}_i = \sum_{j \neq i} \left(\boldsymbol{F}_{ij}^C + \boldsymbol{F}_{ij}^D + \boldsymbol{F}_{ij}^R \right) \tag{1}$$

The conservative force is defined through

$$\boldsymbol{F}_{ij}^C = a_{ij} \omega^C (r_{ij}) \hat{\boldsymbol{r}}_{ij}, \tag{2}$$

where a_{ij} is the repulsive force parameter between particle i and particle j, $\hat{\boldsymbol{r}}_{ij}$ is a unit vector in the direction of $\boldsymbol{r}_{ij}$, ω^C is a weight function and $r_{ij} = \left| \boldsymbol{r}_i - \boldsymbol{r}_j \right|$. The weight function is typically a linear ramp giving rise to very soft repulsive forces. It is the soft nature of the conservative force that allows the use of very large timesteps in DPD compared with molecular dynamics (MD).

The dissipative force depends on both the positions and relative velocities of the particles, $\boldsymbol{v}_{ij}$, through

$$\boldsymbol{F}_{ij}^D = -\zeta \omega^D (r_{ij}) \left(\boldsymbol{v}_{ij} \cdot \hat{\boldsymbol{r}}_{ij} \right) \hat{\boldsymbol{r}}_{ij}, \tag{3}$$

where ω^D is the dissipative weight function, $\boldsymbol{v}_{ij} = \boldsymbol{v}_i - \boldsymbol{v}_j$ and the coefficient ζ controls the strength of the dissipative force. The dissipative force models the viscous drag on a particle due to the surrounding molecules of the fluid represented by the bead.

Thermal noise is introduced by means of a random force of the form

$$\boldsymbol{F}_{ij}^R = \sigma \omega^R (r_{ij}) \xi_{ij} \Delta t^{-1/2} \hat{\boldsymbol{r}}_{ij}, \tag{4}$$

where σ is a parameter that determines the magnitude of the random pair force between the particles, ω^R is the random force weight function, ξ_{ij} is a Gaussian distributed random variable, and Δt is the integration time step.

A requirement that the DPD system corresponds to a statistical mechanical canonical ensemble [2] places a restriction on the choice of weight function and parameters for the dissipative and random force terms; the canonical distribution function will only be a steady state solution of Liouville's equation if the following relationships are obeyed

$$\omega^D = (\omega^R)^2 \tag{5}$$

$$\sigma^2 = 2k_B T\zeta \tag{6}$$

We note here that the above conditions do not imply that DPD is a Hamiltonian system as has been previously suggested [11]. There is no known Hamiltonian from which the DPD equations of motion can be derived. The existence of a Hamiltonian is a sufficient but not necessary condition for the phase space compression factor to vanish [12].

The combination of random and dissipative forces acts as a thermostat in DPD. The random force term tends to heat the system up, while the dissipative term damps out any increase in temperature.

It is customary to make the following choice for the weight functions

$$\omega^C(r_{ij}) = \omega^R(r_{ij}) = \begin{cases} 1 - r_{ij}/r_c & r_{ij} \le r_c \\ 0 & r_{ij} > r_c \end{cases} \quad (7)$$

where r_c is the interaction range or cut-off distance which defines the length scale in DPD. The dissipative weight function follows from Eq. (5).

III. PARAMETERIZATION OF THE CONSERVATIVE FORCES

There are 3 parameters to determine in the DPD simulation of a 1-component system of (monomeric) beads, a, σ and ξ, which become three $m \times m$ matrices upon generalizing to an m-component mixture. The most important of these parameters is the conservative force parameter since it contains all the chemical details of the substance to be modelled; the noise and dissipative parameters are related respectively, to the system temperature, and fluid viscosity. In what follows we shall assume literature values for the damping and noise parameters and focus solely on the choice for the magnitude of the conservative parameter [3].

For 1-component DPD simulations, Groot and Warren have shown that there is a simple relationship between the conservative force parameter and the inverse isothermal compressibility [3]. This relationship is a consequence of the quadratic equation of state for the DPD fluid. As DPD of 1-component systems is of limited interest we shall focus on parameterization of mixtures. To keep the algebra simple, we restrict ourselves to binary systems. Generalisation to more than 2 components is straightforward.

A. Free energy of mixing for a mixture of DPD particles

We now derive an expression for the free energy of mixing of two DPD fluids starting from the equation of state. Both GW [3] and Maiti and McGrother [13] have also derived expressions for the free energy of mixing of binary DPD systems but these authors work with a free energy density, taking a less detailed and transparent approach than ours.

The pressure for a binary mixture of fluid components may be given in terms of partial radial distribution functions by a straightforward generalization of the virial equation, which follows from classical statistical mechanics of systems with pairwise additive potentials [14]

$$P = \rho k_B T - \frac{2\pi}{3}\rho^2 \begin{bmatrix} x^2 \int_0^\infty g_{11}(r) \frac{du_{11}(r)}{dr} r^3 dr + 2x(1-x) \int_0^\infty g_{12}(r) \frac{du_{12}(r)}{dr} r^3 dr \\ +(1-x)^2 \int_0^\infty g_{22}(r) \frac{du_{22}(r)}{dr} r^3 dr \end{bmatrix} \qquad (8)$$

where x is the composition variable, g_{ij} are the partial radial distribution functions, ρ is the total number density of the mixture, and $u_{ij}(r)$ is the pair potential for species i and j.

If we now introduce the DPD conservative force expression (employing a linear weight function) supplemented by the requirement that all species have the *same* interaction range, r_c, Eq. (8) becomes

$$P = \rho k_B T + \frac{2\pi}{3}\rho^2 \begin{bmatrix} x^2 a_{11} \int_0^{r_c} (1 - r/r_c) r^3 g_{11}(r) dr + 2x(1-x) a_{12} \int_0^{r_c} (1 - r/r_c) r^3 g_{12}(r) dr \\ + (1-x)^2 a_{22} \int_0^{r_c} (1 - r/r_c) r^3 g_{22}(r) dr \end{bmatrix} \quad (9)$$

We now transform the integrals by removing the dependence on the interaction range by introducing the quantity $\bar{r} = r/r_c$. This now gives

$$P = \rho k_B T + r_c^4 \rho^2 \left[x^2 a_{11} \alpha_{11} + 2x(1-x) a_{12} \alpha_{12} + (1-x)^2 a_{22} \alpha_{22} \right], \quad (10)$$

where we have also defined the following parameters [13]:

$$\alpha_{ij} = \frac{2\pi}{3} \int_0^1 (1 - \bar{r}) \bar{r}^3 g_{ij}(\bar{r}) d\bar{r} . \quad (11)$$

We note that Eq. (10) describes a *quadratic* equation of state. As pointed out by Pagonabarraga and Frenkel [10], such an equation of state will be produced no matter what choice of weight function is employed. For this reason, the GW form of DPD is inadequate for modelling vapour-liquid equilibria in pure substances.

To a good level of approximation the α's can be taken to be independent of the total density [13] (by virtue of removing the dependence on r_c) and furthermore that $\alpha_{11} \approx \alpha_{12} \approx \alpha_{22} \equiv \alpha$. This last identity is not as serious an assumption as might be thought; it could easily be relaxed if the α_{ij}'s are absorbed into the definition of the a_{ij} parameters. Finally, we may write for the pressure of the DPD mixture,

$$P = \rho k_B T + r_c^4 \rho^2 \alpha \left[x^2 a_{11} + 2x(1-x) a_{12} + (1-x)^2 a_{22} \right]. \tag{12}$$

An equation of state of this form may be integrated using the general limit theorem [15] to give the Helmoltz free energy of the binary mixture [16]

$$A_{mix} = \int_V^\infty \left[P - \frac{n_T RT}{V} \right] dV - RT \sum_i n_i \ln \frac{V}{n_i RT} + \sum_i n_i \left(u_i^0 - T s_i^0 \right) \tag{13}$$

where the lower case letters denote extensive quantities per mole of substance while the '0' superscripts refer to a pure ideal gas reference state. In particular, n_T is the total number of moles, s and u are the molar entropy and molar internal energy, respectively.

Substitution of Eq. (12) (the DPD equation of state) into Eq. (13) gives the Helmoltz free energy per mole of mixture, A_{mix}/n_T, as

$$\frac{A_{mix}}{n_T} = -RT \sum_i x_i \ln \frac{V}{n_i RT} + \sum_i x_i \left(u_i^0 - T s_i^0 \right) + \frac{1}{n_T} \int_V^\infty P_{vir} \, dV \tag{14}$$

where P_{vir} is defined by

$$P_{vir} = \frac{r_c^4 n_T^2 N_A^2 \alpha}{V^2} \left[x^2 a_{11} + 2x(1-x) a_{12} + (1-x)^2 a_{22} \right] \tag{15}$$

Evaluating the definite integral in Eq. (14) gives the following expression for the free energy per mole of mixture

$$\frac{A_{mix}}{n_T} = -xRT\ln\frac{V}{n_1RT} - (1-x)RT\ln\frac{V}{n_2RT} + x\left(u_1^0 - Ts_1^0\right) + (1-x)\left(u_2^0 - Ts_2^0\right) + \frac{r_c^4 n_T N_A^2 \alpha}{V}\left[x^2 a_{11} + 2x(1-x)a_{12} + (1-x)^2 a_{22}\right] \tag{16}$$

The free energy of mixing, A^M, is obtained by subtracting the free energies of the two pure components from that of the mixture [17]:

$$\frac{A^M}{n_T} = \frac{A_{mix}}{n_T} - x\frac{A_1}{n_1} - (1-x)\frac{A_2}{n_2} \tag{17}$$

where A_1 and A_2 are the free energies of pure components 1 and 2 respectively. These pure component free energies can be obtained from the free energy of the mixture by using the molar volume of the pure species in place of the total molar volume and setting the mole fraction x to unity and zero for species 1 and 2, respectively. These free energies per mole of each substance are

$$\frac{A_i}{n_i} = -RT\ln\frac{V_i}{n_iRT} + \left(u_i^0 - Ts_i^0\right) + \frac{r_c^4 n_i N_A^2 \alpha\, a_{ii}}{V_i}, \tag{18}$$

in which the subscript i refers to substance 1 or 2. The Helmoltz free energy of mixing, A^M , is then given by

$$\frac{A^M}{n_T} = xRT\ln\left(\frac{xv_1}{v}\right) + (1-x)RT\ln\left(\frac{(1-x)v_2}{v}\right)$$
$$+\frac{r_c^4 N_A^2 \alpha}{v}\left[x^2 a_{11} + 2x(1-x)a_{12} + (1-x)^2 a_{22}\right] \qquad (19)$$
$$-x\frac{r_c^4 N_A^2 \alpha\, a_{11}}{v_1} - (1-x)\frac{r_c^4 N_A^2 \alpha\, a_{22}}{v_2}$$

in which we have introduced the molar volumes in place of the extensive total volumes. The first two terms on the *rhs* of Eq. (19), having an explicit temperature dependence, may be regarded as the entropic contribution to the free energy of mixing. Introducing the volume fractions

$$\phi_1 = \frac{V_1}{V} \equiv \frac{x_1 v_1}{v} \equiv \phi, \qquad (20)$$

in which we have assumed (as in regular solution theory) that there is no volume change upon mixing (partial molar volumes are equal to the molar volumes). This leads to an entropy of mixing per mole of the mixture of

$$\frac{s^M}{R} = -x\ln\phi - (1-x)\ln(1-\phi) \qquad (21)$$

Eq. (21) is very similar to the expression for the ideal entropy of mixing, becoming exactly so when the volume fractions and mole fractions coincide, which happens for components which have equal molar volumes.

The remaining contribution to the free energy of mixing, which we shall loosely call the excess free energy of mixing (excess properties of mixing are usually defined relative to the properties of an ideal mixture at the same temperature, pressure and composition) is from Eq. (19)

$$\frac{A^E}{n_T} = -r_c^4 \nu N_A^2 \alpha \left[\frac{a_{11}}{v_1^2} - 2\frac{a_{12}}{v_1 v_2} + \frac{a_{22}}{v_2^2} \right] \phi(1-\phi) \tag{22}$$

We note here that Groot and Warren derived an expression for the free energy of mixing in which the entropy term was ideal and the heat term was given in terms of mole fractions [3], while Maiti and McGrother did not consider the entropy of mixing and also derived a heat of mixing which was quadratic in mole fraction, not volume fraction [13].

B. Mapping DPD onto Regular Solution Theory

Equation (22) derived in the last section has almost the same form as the free energy of mixing derived by Scatchard [18] and Hildebrand [19] for systems described as regular mixtures by Hildebrand [20]. Hildebrand defined a regular solution as one in which the excess entropy, S^E, and excess volume, V^E, of mixing are both zero. Regular mixtures display positive deviations from Raoult's law and are typically formed from components with non-polar molecules (essentially ignoring dipolar and hydrogen bonded forces between molecules). Scatchard and Hildebrand obtained the following equation for the excess energy of mixing, u^E,

$$u^E = v\,(c_{11} + c_{22} - 2c_{12})\phi(1-\phi) \equiv g^E \tag{23}$$

where the last identity in Eq. (23) follows from $V^E = S^E = 0$, and the parameters c_{11} and c_{22} are the cohesive energy densities of the two pure liquids defined by

$$c \equiv \frac{\Delta_{vap}u}{v^L} \tag{24}$$

in which $\Delta_{vap}u$ is the molar internal energy of vaporisation and v^L is the molar volume of the liquid. The main assumptions used to derive Eq. (23) are that $V^E = 0$ and that the energy of the binary mixture can be expressed as a quadratic function of the volume fraction [17]. Eq. (23) can also be viewed as the leading term in the Redlich-Kister expansion of the excess free energy of mixing where the 3 terms in parentheses are then lumped together to form a new empirical constant, A. The assumption of zero excess entropy is true for only a few non-ideal mixtures and for this reason, the term 'regular mixture' is reserved in more modern treatments for those mixtures for which the constant A in the Redlich-Kister expansion is temperature independent [21]. Nevertheless, many mixtures can be adequately represented by Scatchard and Hildebrand's regular solution theory due in part to a fortuitous cancellation of errors. Their theory is also quite simple to understand and provides meaningful physical insight, which is lacking in the more empirical treatments of the free energy of mixing. It is advantageous to make a correspondence between DPD and regular solution theory since there is then a direct link

between the conservative interaction parameters, a_{11} and a_{22} and the cohesive energy densities, c_{11} and c_{22}.

GW [3] and Maiti and McGrother [13] used similar arguments to develop equations for the free energy density of DPD particles in a binary mixture. They arrived at a similar expression (though see earlier note on this) to Eq. (22), suggesting a correspondence with the Flory-Huggins lattice theory of polymeric solutions. Through our detailed derivation of the thermodynamics of mixing we have shown that the correspondence is closer to that of regular solution theory. It should be noted that in Flory-Huggins theory, the *same* form of the heat of mixing (as in RST) is employed; the significant difference lies in the treatment of the entropy of mixing. By focussing on FH theory both sets of authors missed the link between the like-like interaction parameters and cohesive energy density. Instead, they set $a_{11} = a_{22}$ whose value they suggested could be determined from the isothermal compressibility (as for the 1-component DPD case). This was an unfortunate oversight; the use of equal like-like interactions is only justified in a few special cases and will not in general give rise to the expected phase behaviour.

The cross interaction parameter c_{12} was related to c_{11} and c_{22} in Hildebrand's theory by a geometric mean,

$$c_{12} = \sqrt{c_{11}c_{22}} \tag{25}$$

which has some physical justification for non-polar molecules based on London's dispersion force formula, but is only approximately true. Use of Eq. (25) gives the

following expression for the excess free energy of mixing in regular solution theory (RST), g^E_{RST},

$$g^E_{RST} = v\,\phi(1-\phi)\left(\delta_1 - \delta_2\right)^2, \tag{26}$$

in which δ_1 and δ_2 are now the square roots of the pure component cohesive energy densities, or the Hildebrand *solubility parameter*. Comparing Eq. (22) with Eq. (26) gives the following mapping between the DPD parameters and cohesive energy densities,

$$\left(\delta_1 - \delta_2\right)^2 = -r_c^4\alpha\left[\rho_1^2 a_{11} + \rho_2^2 a_{22} - 2\rho_1\rho_2 a_{12}\right] \tag{27}$$

The negative sign on the *rhs* of Eq. (27), which arises from the use of a purely repulsive conservative force, is significant; without it there would be a one to one correspondence between a_{11} and δ_1, and between a_{22} and δ_2 with a_{12} then given by the geometric mean of a_{11} and a_{22}. Instead we must regard Eq. (27) as a definition of a_{12}. This is possible since all other parameters are in principle known: a_{11} and a_{22} could be determined from pure component compressibility data as suggested by GW, while α has been determined by the same authors to be approximately 0.1 for DPD densities $\rho r_c^3 > 3$. Alternatively, we propose that a_{11} and a_{22} be determined from Hildebrand solubility parameters via the following argument. The cohesive energy density is approximately equal to the volume derivative of the internal energy (internal pressure),

$$\frac{E_{coh}}{V} \equiv \delta^2 \approx \frac{\partial U}{\partial V} \tag{28}$$

This relationship is exact for a van der Waals fluid. The internal pressure is given by the thermodynamic equation of state as

$$\frac{\partial U}{\partial V} = T\frac{\partial P}{\partial T} - P \tag{29}$$

The only explicit temperature dependent part of the DPD pressure equation of state involves the ideal gas contribution, therefore the internal pressure is just the virial term with its sign reversed. Hence using Eqs. (15, 28 & 29) and setting the mole fraction to be 1 or 0, we obtain

$$a_{ii} = \frac{\delta_i^2}{\alpha \rho_i^2 r_c^4} \tag{30}$$

Solubility parameters have been determined for a wide range of substances including solids. For a substance which is a solid at the temperature of interest, one uses the molar volume of the subcooled liquid to calculate the solubility parameter [20]. The most reliable method of calculating these parameters is to use Eq. (24) in which the heat of vaporisation is required [20]. Various other methods are available for calculating or estimating solubility parameters including estimation from the Hildebrand rule, from critical constants or surface tension. Many of these methods are described in the textbook

by Hildebrand and Scott [20]. To complete the parameterization of the conservative forces one must specify the value of r_c, which we will discuss in the following section.

IV DPD SIMULATION OF A 2-COMPONENT MIXTURE

To validate the new parameterization of the conservative forces we have conducted a series of DPD simulations in which we have modelled the phase equilibrium of a 2-component mixture of inorganic species. We have chosen to study the system $SiCl_4/SnI_4$ for several reasons: First, it is far removed from polymer systems and therefore illustrates the wide applicability of our new parameterization; Second, this system is known to behave as a regular mixture; Third, experimental solubility data are available for this system; Finally, the mixture phase-separates below 140°C, forming two liquid phases with a non-symmetric composition, providing a stern test of the new parameterization.

A. Experimental data

Hildebrand and Negishi have determined the solubility of SnI_4 in a $SiCl_4$ solvent at a set of temperatures ranging from 0.2 °C to just below 140 °C [9]. From this data they derived a set of values for the square difference in solubility parameters, $\left(\delta_{SnI_4} - \delta_{SiCl_4}\right)^2$ at various temperatures by applying the RST derived equation for the activity coefficient of SnI_4. Molar volumes, used in the RST fit, were extrapolated from experimental data

obtained by other authors, while the ideal solubilities of solid SnI_4 in liquid $SiCl_4$ were calculated using measured values of the heat of fusion and molar excess heat capacity of the liquid over the solid phase.

We have used Hildebrand and Negishi's derived $\left(\delta_{SnI_4} - \delta_{SiCl_4}\right)^2$ data together with Eq. (26) to calculate the excess free energy per mole of the mixture as a function of temperature. By adding the entropic contribution, we calculated the molar free energy of mixing. This data was then used with the thermodynamic software code, Thermo-Calc to determine the locus of coexisting solubilities (the binodal phase boundary). The calculated phase boundary is a skewed parabola with a maximum at about 144˚C, occurring at a composition of around 44 mole percent of SnI_4. It should be noted that the right hand branch of the *T-x* diagram is obtained by extrapolating far beyond the range of experimental solubility data and must therefore be seen only as a guide (see later plot in Fig. 4). The upper critical solution temperature (UCST) is overestimated by Thermo-Calc; this can be taken as a measure of the error in applying RST to this system

To conduct our DPD mixture simulations we require a set of data for the solubility parameters of each of the pure components as a function of temperature in order to fully parameterise the conservative force matrix. There are several ways to proceed from here but we have chosen to do the following: (1) Calculate a value of the solubility parameter for $SiCl_4$ at 25 ˚C and then extrapolate to obtain values at the other temperatures; (2) The solubility parameters for SnI_4 are then calculated using these values together with Hildebrand and Negishi's values for $\left(\delta_{SnI_4} - \delta_{SiCl_4}\right)^2$ at each of the temperatures.

An alternative approach would be to calculate directly the SnI_4 solubility parameters using extrapolated vaporization enthalpies. However, SnI_4 is a solid across much of the temperature range and hence introduces the added difficulty of having to determine values for the molar volume and heat of vaporization for the subcooled liquid.

The first step in our chosen scheme involves calculating the solubility of $SiCl_4$ at 25 ˚C. This we determined from a tabulated value of the standard enthalpy of vaporisation at this temperature, $\Delta_{vap}h^{298}$ of 29.7 kJ mol^{-1} [22], together with the equation

$$\delta_{SiCl_4} \cong \left(\frac{\Delta_{vap}h[SiCl_4] - RT}{v_{SiCl_4}} \right)^{1/2}, \tag{31}$$

which follows from Eq. (24) upon assuming the vapour behaves as an ideal gas [20]. A more sophisticated calculation should involve the compressibility factor of the vapour [20]. Solubility parameters at the remaining temperatures of interest were also determined using Eq. (31), but now with values of the enthalpy of vaporisation estimated at these temperatures from Kirchhoff's law,

$$\Delta h(T_2) = \Delta h(T_1) + \int_{T_1}^{T_2} \Delta c_p dT \tag{32}$$

where c_p is the constant pressure molar heat capacity and T_1, T_2 are the two temperatures of interest. For the particular case of the heat of vaporisation, provided the heat capacity of the liquid and vapour phases can be taken to be approximately independent of temperature, we may write

$$\Delta_{vap}h(T_2) = \Delta_{vap}h(298K) - \Delta c_p(T_2 - 298.15K) \tag{33}$$

where Δc_p is now the difference between the molar heat capacity of the liquid and vapor phases, and the reference temperature is taken to be 298 K. Taking a value for $C_p(SiCl_4, liq) = 145.3$ J K^{-1} mol^{-1} and $C_p(SiCl_4, gas) = 90.3$ J K^{-1} mol^{-1} [22] gives $\Delta C_p = 55$ J K^{-1} mol^{-1}.

The next stage of the parameter determination is to estimate a set of solubility parameters for SnI_4. This was achieved by using

$$\delta_{SnI_4} = \delta_{SiCl_4} + \sqrt{\left(\delta_{SnI_4} - \delta_{SiCl_4}\right)^2} \tag{34}$$

The values we obtained for the heat of vaporization and solubility parameters are collected in Table 1.

B. DPD simulation details

DPD simulations are commonly conducted using a system of dimensionless units. The interaction distance, r_c is an obvious choice for the unit of length while the mass of the DPD beads can be used as the unit of mass. One choice for the unit of energy is the value of k_BT. With these three choices, the timestep is then determined. Another possibility would be to choose a suitable unit of time, which would then set the energy scale. We have opted for the former method in view of its simplicity. In this system we define a set of dimensionless quantities that we henceforth denote using an overbar. For

example, the dimensionless number density, $\overline{\rho} = \rho r_c^3$, while the repulsive parameters become, $\overline{a}_{ij} = a_{ij} r_c / (k_B T)$.

Defining an energy scale based on $k_B T$ means the repulsive parameters become temperature dependent and further, that the DPD simulations are all conducted at unit temperature; separate DPD simulations must be conducted to explore different real temperatures. There is an effective lower limit to the reduced DPD density; GW determined that $\overline{\rho} \geq 3$ in order for a quadratic equation of state to be recovered that is independent of the magnitude of the conservative force parameter. Employing higher values of density than this will increase the computing overheads of a simulation hence it is desirable to keep it as close to 3 as possible. Fixing the reduced density effectively sets the value of r_c since it is then given by the cube root of three times the reciprocal of the density of the substance of interest. Note that this interaction length can be increased but only at the cost of increasing the value of the reduced density. Some authors introduce an extra parameter involving the number of atoms that a DPD bead is supposed to represent to act as an extra scaling factor on r_c, allowing it to increase, while keeping the reduced density constant. We have chosen not to adopt this approach and hence our version of DPD does not run into problems such as those discussed in the article by Pivkin and Karniadakis, in which the DPD fluid solidifies beyond a certain level of coarse graining [23]. This leaves open the question of what the DPD beads represent. We have taken the view that the beads are blobs of fluid (see the article by Kim and Phillips for a very illuminating and insightful description of what the DPD particles represent [24]). By insisting that the beads all have the same interaction range, r_c, all we are saying is that when two such beads represent either different substances under similar thermodynamic

conditions or different thermodynamic states of the same substance, the volume of each bead simply encloses a different number of atoms or molecules; for a vapor there will be far fewer molecules in such a control volume than for the same substance under conditions in which it is a liquid. Clearly, in this example, the 'vapor' beads must have a softer interaction than the 'liquid' beads, but this is accounted for in the value of the conservative force parameter, which will be greater (more repulsive) for the "liquid" beads. Beads representing lumps of a solid phase will have even higher repulsive parameters due to the higher density of the underlying atomic units. It is useful to think of the DPD beads as representing "spheres of influence" of the underlying molecules with a size that is characterised by a diameter, r_c.

For simplicity, our mixture simulations have all been conducted at the equimolar composition. The mixture volume is then given by the arithmetic mean of the pure component molar volumes (we assume here, as in RST, that the partial molar volumes differ very little from the pure component molar volumes). The number density of these mixtures at the various temperatures is then calculated by multiplying the reciprocal volume of one mole of the mixture (its molar density) by the Avogadro constant.

In order to satisfy both the requirement of having a constant r_c for all our simulations and having a reduced density as close as possible to 3, we have fixed the value of r_c based on the largest value of any pure component molar volume across the range of temperatures under investigation. In our case the highest value of molar volume occurs at the temperature of 139.9 ˚C for $SiCl_4$. This gives a value of r_c = 0.9362 nm. With this choice, the reduced density of all our mixtures stays close to 3 and never dips below it.

Once the values of the dimensionless solubility parameters have been determined using the above choice for the interaction range, the repulsive parameters are then obtained with the aid of Eq. (30) together with the dimensionless version of Eq. (27). The variation of these parameters with temperature is shown in Fig. 1. The graph shows that the parameters decrease with increasing temperature, as expected. Furthermore, it can be seen that the parameters for a pair of interacting SnI_4 beads are greater than for $SiCl_4$ beads. This is sensible since SnI_4 is almost 3 times as dense as $SiCl_4$ at 25 ˚C, being a solid at this temperature. The mixing term falls somewhere in between the two like-like parameter values.

Simulations were solved using a DPD code that implements the standard GW method supplied by Accelrys Inc. [25]. Cubic boxes, with imposed 3D periodic boundary conditions, containing random arrangements of between 24400 and 30890 beads were simulated for an equilibration phase of 100,000 steps followed by a production phase comprising of 100,000 steps. Equilibrium was deemed to have been achieved when the cumulative average temperature and pressure reached a plateau. A time step of $\Delta\bar{t} = 0.02$ was used throughout and the values of the noise and damping coefficients were $\bar{\sigma} = 3$ and $\bar{\xi} = 4.5$, respectively. The DPD simulations may be thought of as being equivalent to a quench from a high configurational temperature (random arrangement of beads) to thermodynamic equilibrium at the temperature of interest, under constant volume conditions.

V. RESULTS AND DISCUSSION

By viewing snapshots taken from the simulations it was possible to discern clear $SiCl_4$ rich zones, and SnI_4 rich zones at low temperatures indicative of the early stages of phase separation. As temperature approached the experimental critical point the snapshots showed little evidence of any phase separation. Due to the ambiguity of snapshots we have chosen not to present them in this manuscript. To determine the composition of two coexisting phases we could perform the simulations in an elongated box using a large value of the Flory-Huggins coefficient to promote phase separation with a stable planar interface as used in the paper by GW. However, we have chosen not to follow this method because (a) it is not necessary to wait until complete phase separation takes place, (b) we wish to show that the DPD mixture will phase separate at the points where the experimental system phase separates (which should occur if the parameterization is correct) and not simply at some mean field value.

As remarked above the simplest approach to analysing phase equilibria without ensuring one has a planar interface entails calculating distribution functions of local densities and compositions. This method relies on the fact that these local distributions reach equilibrium much faster than the time taken to achieve global equilibrium.

To use this method, one first constructs a histogram of the local density; different phases will then appear as separate peaks in the histogram. The local density can be calculated by dividing up the simulation box into a smaller number of cubes of equal volume and then simply counting the number of beads that lie within the region enclosed by each one. However, two coexisting phases cannot occur without the creation of an interface

between them. For a relatively small total number of particles, a significant number of these will reside in the interfacial region. The naïve local density approach described above will lead to a smeared out histogram as a result of the contributions of the sub-cubes located in the interfacial region [26]. A better strategy than this involves identifying those sub-cubes which reside in the interfacial region, and removing these from the statistical analysis. Gelb and Müller have devised a simple scheme by which the phase boundary can be easily located [26]. Their method entails forming a histogram of local coordination number or better still, a histogram of component specific coordination number. This histogram is obtained by first selecting a cutoff distance, then determining the number of neighbours (or neighbours of a given species) of each bead in the simulation box. From the histogram that is produced, one may determine a criterion for deciding which beads belong to the interfacial region. For a two phase system, such a histogram will be bimodal; the higher density phase will be characterised by beads with relatively high coordination numbers, while the lower density phase will give rise to a peak at relatively low coordination numbers. Beads that lie in the interfacial region will be characterised by having coordination numbers intermediate between the average values for the two phases. Having defined a region of coordination numbers that constitutes membership of the interfacial region, one then determines which of the original set of sub-cubes are to be excluded from the analysis. We have followed Gelb and Müller by deeming a sub-cube to be interfacial if more than 30% of its constituent beads are themselves interfacial by virtue of the coordination number analysis. It should be stressed that the above local density scheme is carried out post-process and in no way affects the performance of the DPD simulations. Furthermore, it may be parallelised.

The choice of which cutoff distance to employ is somewhat arbitrary. However, choosing a value too low will give poor resolution of the two coexisting phases while too high a value will give an interface that is too "thick". The choice for the number of sub-cubes to use in the local density calculation is also somewhat arbitrary. In our simulations we typically used a discretization of 7×7×7 sub-cubes but the highest discretization used 8×8×8 cubes. These numbers were determined by trial and error – too few cubes gave poor resolution of the two peaks in the density profile while too high a value resulted in too few particles per cube to calculate a meaningful average local density. For the coordination analysis we used cutoff distances ranging from 1.25 at 0 ˚C to 2.0 at 131 ˚C. We opted to calculate the coordination number of $SiCl_4$ beads around any given bead regardless of its own identity. This choice gave a clearer separation of the peaks in the histogram for a smaller cutoff than one based upon a "species blind" coordination number histogram. During the DPD simulations, several snapshots were taken at equally spaced intervals of time. Our statistical analysis was carried out on each of the snapshots and the results averaged in the final analysis.

A set of density histograms are shown in Figs. 2a-e. These histograms have been obtained via the method outlined above. The histograms below 140 ˚C are bimodal with a peak centred on a density of around $\overline{\rho} = 3$, largely independent of temperature and a second peak that moves inwards towards lower densities with increasing temperature. At the lowest temperature plotted (0 ˚C) the second peak lies at a density of around 6, a factor of two greater than the mean density of the 1st peak.

We can interpret the results plotted in Fig. 2 in the following way. As temperature increases we expect more of the SnI_4 to dissolve in the $SiCl_4$ liquid phase. The $SiCl_4$ rich

phase will become less dense (when measured in DPD units) because the SnI_4 beads are much more repulsive between themselves and the $SiCl_4$ beads, than the $SiCl_4$ beads are between themselves. This causes the $SiCl_4$ rich phase to expand in volume, thus lowering its density. Once all of the solid SnI_4 has melted we are left with two coexisting liquids with densities that are not sufficiently different to separate by the local density histogram method we have employed. As the critical temperature is reached, it becomes impossible to discern two phases; plots of coordination number show only a single peak no matter what cutoff is chosen. This is not a concern in the present context since we are not interested in accurately determining the critical temperature or composition. The species coordination number histograms are shown in Fig. 3 for sub-set of the temperatures studied. This plot illustrates how the peaks merge together as the critical temperature is approached. To resolve the phases in the vicinity of the critical point requires the use of a more sophisticated technique than we have employed. Methods which are based on topology, such as the use of ring statistics frequently employed in simulations of network glasses, may be useful in this context.

Once the two coexisting phases have been identified from an inspection of the local density histogram, the mean values of the density and composition of each phase can be determined. For a given temperature we obtain two values for the composition which can then be plotted to yield the binodal phase boundary. Each of these points is the result of averaging the composition from 5 individual snapshots taken at regular intervals during the last phase of the DPD production runs. Errors were calculated based on one standard deviation from the mean values and were typically smaller than the plot symbols. However, by far the largest sources of error will come from the approximations

that we have made in the parameterization (use of constant heat capacities, assumption of ideal vapour phase, assumption of zero volume change on mixing, errors in the original experimental data etc.).

The results from our analysis (solid circles) are plotted against the Thermo-Calc generated phase boundary data (crosses) and Hildebrand and Negishi's experimental solubility data on a *T*-*x* diagram shown in Fig. 4. It is clear from Fig. 4 that the results for the $SiCl_4$ rich phase are in excellent agreement with the experimental data until we enter the two liquid region where the single DPD data point in that regime appears at too high a temperature. We attribute this to the difficulty in resolving the two liquid phases using our simple histogram method. The Thermo-Calc results are shifted to the right of the DPD and experimental data. This systematic discrepancy is the result of the approximations employed in RST. Lack of experimental data on the SnI_4 rich phase mean that the DPD and Thermo-Calc data are at best a crude guide to the true phase behaviour. Nevertheless, the agreement between Thermo-Calc and DPD is encouraging.

Finally we have conducted three additional DPD simulations using the parameterization scheme commonly employed by many DPD practitioners. For these simulations we set $\bar{a}_{11} = \bar{a}_{22} = \bar{a} = 25$ but determined the value of $\bar{a}_{12}$ using the RST calculated heat of mixing (equivalent to using what GW call the Flory-Huggins coefficient). Using our Eq. (27) we may write (in the spirit of these other DPD authors),

$$\left(\bar{\delta}_1 - \bar{\delta}_2\right)^2 = 2\alpha\bar{\rho}^2\left(\bar{a}_{12} - \bar{a}\right). \tag{35}$$

We carried out these extra DPD runs at temperatures, 25 ˚C, 88 ˚C and 139.9 ˚C. Using Eq. (35) together with the solubility parameters taken from Table 1, we obtained the following respective set of values for $\bar{a}_{12}$: 31.4, 30.0, 28.5 using a $\bar{\rho} = 3$ and a value of r_c = 0.87 nm. Random configurations of equimolar mixtures of beads were equilibrated in exactly the same manner as in our main simulation work (system size was 24000 beads in each case). After a production phase, the snapshots obtained from the last trajectory were stored to disk and these were then analysed.

All three snapshots looked very similar and it was impossible to discern any phase separation by visual inspection. Local coordination number histograms were all single humped regardless of the cutoff employed. Local density histograms were therefore calculated without the clean-up procedure described earlier. These histograms are plotted in Fig. 5 for a discretization of 7×7×7 sub-cubes. It is clear from Fig. 5 that there is no evidence for the existence of two coexisting phases at any of the 3 temperatures. Wijmans and co-workers determined that for the system with $\bar{a}_{11} = \bar{a}_{22} = 25$ and a DPD density of 3, phase separation cannot be expected until $\bar{a}_{12}$ is somewhere between 28.5 to 31.4 in value[27]. Since this value is larger than the ones we used in our three simulations it would seem an unfair criticism. However, the point is that if DPD is to be taken seriously, then a well parameterised model must predict phase separation at a point coincident with experiment. Evidently, this is not true of the established parameterization method.

A parameterization of soft-core potentials typically employed in DPD and based on equal diagonal elements of the force parameter matrix, is known to yield fluid-fluid phase separation in binary mixtures. Such an approach is appealing since it can act as a crude model of binary polymer solutions (see for example Finken *et al* [28] and Archer and

Evans [29]). However, these parameterizations are tied to mean field Flory-Huggins theory and may only give rise to symmetric coexistence curves. Maiti and McGrother added a proof of why $\bar{a}_{11} = \bar{a}_{22}$, based on a thought experiment [13]. This proof is based on the conjecture that both components must have equal molar volumes, which is not true in general and seems to be a consequence of the Flory-Huggins lattice theory. It is clearly more desirable to have a parameterization method which is mapped to real experimental data, is not restricted to polymers or mean field theory, and can be used in a predictive sense.

VI. CONCLUSIONS

We have introduced a significantly improved method of parameterizing the Groot-Warren formulation of Dissipative Particle Dynamics (DPD) by exploiting a correspondence with Scatchard-Hildebrand regular solution theory. Using thermodynamic arguments we have shown that the free energy of mixing of a DPD mixture has almost the same form as that derived using RST. The central difference lies in the entropy of mixing. In the case of DPD, we find that the entropy of mixing is greater than that of an ideal mixture when the molar volumes of the two components are not equal. In fact, our entropy of mixing expression is formally identical to one derived by Hildebrand for athermal mixtures using the concept of free volume, and also in agreement with the entropy of mixing of polymer solutions derived by Flory [20]. RST, on the other hand, assumes the excess entropy of mixing is zero. Significantly, the heat of mixing of two DPD fluids has exactly the same form as that in RST, being a quadratic

function of the volume fractions. Using this correspondence we have established that the self-interaction parameters are related to the cohesive energies of the pure fluids and have derived a method of obtaining them. This is a significant departure from what has previously been practised in the DPD literature, where the self-interaction terms are typically taken to be equal. Some exceptions have been made to this rule, when simulations have involved molecules with hydrophilic heads and hydrophobic tails for example, but the variation in parameters has been somewhat arbitrary. By contrast, we now provide a physical basis for establishing the magnitude of the self-interaction parameters. For the cross interaction parameters we do not take the more drastic step of assuming they obey a geometric mean combining rule as per RST. Instead, we used an RST-derived heat of mixing (which *does* involve the use of the geometric mean rule) to define these parameters. This may seem like a subtle difference, but it means DPD is not intimately tied to RST; experimental data on heats of mixing could be used in place of one based on a geometric mean combining rule. It is also worth noting that molecular simulation methods, such as Molecular Dynamics and Monte Carlo, frequently employ the Lorentz-Berthelot combining rules, and thus are not immune from this problem, which arises from the lack of an accurate theory of the interaction energy of a pair of chemically dissimilar molecules.

We have validated our new parameterization scheme by modelling the binary system: $SnI_4/SiCl_4$, which displays liquid-liquid coexistence below an upper critical solution temperature around 140˚C. A series of DPD simulations were conducted at a set of temperatures ranging from 0˚C to above the experimental upper critical solution temperature using conservative parameters based on extrapolated experimental data.

These simulations can be regarded as being equivalent to a quench from a high temperature to a lower one at constant volume.

Our simulations recovered the expected phase behaviour ranging from solid-liquid coexistence to liquid-liquid co-existence, eventually leading to a homogeneous single-phase system. The results yield a binodal curve in close agreement with one predicted using regular solution theory, but, significantly, in closer agreement with actual solubility measurements, suggesting the DPD system is an improvement over RST. This last point means that DPD should *not* be regarded as a solver for RST – if that were the case, DPD would be pointless.

To further illustrate the importance of allowing the self-interaction parameters to differ from each other in magnitude, we conducted a series of DPD simulations using the commonly practised procedure of setting these parameters to be equal in magnitude. These simulations demonstrated that the known phase behaviour of $SnI_4/SiCl_4$ could not be recovered.

Regular Solution Theory provides a very convenient framework in which to parameterize the whole conservative force matrix. Particularly useful is the ability of RST to predict the behaviour of mixtures from a knowledge of only the pure components. Furthermore, RST is easily extended to treat multi-component mixtures. The correspondence between DPD and this more general form of RST should be preserved, opening up DPD to simulating more complex solutions.

RST does have some drawbacks and we now consider some of the more serious ones, indicating how these may be overcome. We have already pointed out that while RST assumes $S^E = 0$, DPD does not implicitly assume this. The next assumption, namely

that $V^E = 0$ is implicit in our correspondence between the self-interaction terms and the cohesive energy densities of pure fluids. Fortunately, this assumption has little consequence and can therefore be ignored [20]. More serious is the assumption of the geometric mean combining rule and the restriction of RST to non-polar fluids. However, improvements on the basic RST were introduced early into the development of the theory [30]. The geometric mixing rule can be improved by introducing a correction factor which is then either treated as an empirical constant or approximated from a knowledge of intermolecular forces [17]. To move away from non-polar solutions, one can split up the solubility parameter into 3 separate components: a non-polar, polar and hydrogen bonding term [31]. The DPD conservative force could in principle be similarly sub-divided, and hence the correspondence could be preserved. That leaves the question of determining these 3 components experimentally. Various attempts have been made to determine these parameters with some degree of success and thus tables of their values exist.

Our method of validating the new parameterization of DPD used the phenomenon of phase equilibria as a matter of convenience. However, DPD could turn out to be a powerful tool to *study* phase equilibria, particularly those occurring in confined environments. Methods such as Monte Carlo do not permit a study of the time dependence and hence rule out studying the kinetic aspects of spinodal decomposition. Quench Molecular Dynamics, on the other hand, suffers from time scale issues and it is difficult to see how such a method could be used to study a system as complex as a hydrating Portland cement or a multi-component glass with the complexity of those typically employed in the nuclear industry, for example.

Aside from the potential use of DPD for studying phase equilibria, a whole class of problems concerning the flow of complex mixtures may be tackled by this method. What is lacking at the moment is a deeper understanding of the role of the dissipative force term in determining the fluid viscosity.

In summary, through the definition of the conservative force terms which represent the chemical interactions, and the definition of an unambiguous length scale in terms of the density of the materials being simulated, we believe we have taken a significant step toward developing DPD from its inception as a promising method for mesoscale simulations, towards being a powerful simulation tool with a plethora of interesting applications.

VII ACKNOWLEDGEMENTS

This work has been funded by the Nuclear Decommissioning Authority (NDA), UK. We would like to thank Dr Hajimi Kinoshita for help with Thermo-Calc. Drs Lev Gelb (Washington University, USA) and Eric Müller (Imperial College, UK) are thanked for useful discussions concerning the local density analysis method. Dr Martin Whittle is also thanked for a critical reading of an early version of the manuscript.

References

[1] P. J. Hoogerbrugge and J. M. V. A. Koelman, Euro. Phys. Lett. **19**, 155 (1992)

[2] P. Español and P. B. Warren, Euro. Phys. Lett. **30**, 191 (1995)

[3] R. D. Groot and P. B. Warren, J. Chem. Phys. **107**, 4423 (1997)

[4] M. Kranenburg, M. Venturoli, and B. Smit, Phys. Rev. E **67**, 060901 (2003)

[5] R. D. Groot, T. J. Madden, and D. J. Tildesley, J. Chem. Phys. **110**, 9739 (1999)

[6] S. Yamamoto, Y. Maruyama, and S. Hyodo, J. Chem. Phys. **116**, 5842 (2002)

[7] L. Rekvig, M. Kranenburg, J. Vreede, B. Hafskjold, and B. Smit, Langmuir **19**, 8195 (2003)

[8] A. S. Özen, U. Sen, and C. Atilgan, J. Chem. Phys. **124**, 064905 (2006)

[9] J. H. Hildebrand and G. R. Negishi, J. Am. Chem. Soc. **59**, 340 (1937)

[10] I. Pagonabarraga and D. Frenkel, J. Chem. Phys. **115**, 5015 (2001)

[11] S. M. Willemsen, T. J. H. Vlugt, H. C. J. Hoefsloot, and B. Smit, J. Comput. Phys. **147**, 507 (1998)

[12] D. J. Evans and G. P. Morriss, *Statistical Mechanics of Nonequilibrium Liquids* (Academic Press, London, 1990).

[13] A. Maiti and S. McGrother, J. Chem. Phys. **120**, 1594 (2004)

[14] D. A. McQuarrie, *Statistical Mechanics* (Harper Collins, New York, 1976).

[15] L. J. Gillespie, Chem. Rev. **18**, 359 (1936)

[16] J. A. Beattie, Chem. Rev. **44**, 141 (1949)

[17] J. M. Prausnitz, R. N. lichtenthaler, and E. G. d. Azevedo, *Molecular thermodynamics of fluid-phase equilibria* (Prentice Hall, New Jersey, 1999).

[18] G. Scatchard, Chem. Rev. **8**, 321 (1931)

[19] J. H. Hildebrand and S. E. Wood, J. Chem. Phys. **1**, 817 (1933)

[20] J. H. Hildebrand and R. L. Scott, *The solubility of non-electrolytes* 3rd ed (Reinhold Publishing Corporation, New York, 1950).

[21] J. S. Rowlinson, *Liquids and liquid mixtures* 1st ed (Butterworths Scientific Publications, London, 1959).

[22] *Handbook of Chemistry and Physics*, edited by D. R. Lide (CRC Press, 2002), Vol. 83.

[23] I. V. Pivkin and G. E. Karniadakis, J. Chem. Phys. **124**, 184101 (2006)

[24] J. M. Kim and R. J. Phillips, Chem. Eng. Sci. **59**, 4155 (2004)

[25] Computational results were obtained using software programs from Accelrys. Dissipative Particle Dynamics calculations were carried out using the DPD module of Materials Studio. Structure data files were generated using Materials Studio: Release 4.0, Accelrys Software, Inc.: San Diego, 2006.

[26] L. D. Gelb and E. A. Müller, Fluid Phase Equilibria **203**, 1 (2002)

[27] C. M. Wijmans, B. Smit, and R. D. Groot, J. Chem. Phys. **114**, 7644 (2001)

[28] R. Finken, J.-P. Hansen, and A. A. Louis, J. Stat. Phys. **110**, 1015 (2003)

[29] A. J. Archer and R. Evans, Phys. Rev. E **64**, 041501 (2001)

[30] J. H. Hildebrand, Proc. Natl. Acad. Sci. USA **76**, 6040 (1979)

[31] C. M. Hansen, J. Paint Tech. **39** (1967)

Table 1. Hildebrand solubility parameters for $SiCl_4$ and SnI_4 derived from extrapolated heat of vaporisation data, together with experimental data on the molar volumes and square of the solubility parameter differences. Experimental data taken from Ref. [9].

t / °C	v_{SnCl4} /cm^3 mol^{-1}	v_{SnI4} /cm^3 mol^{-1}	$(\delta_{SnI4}-\delta_{SnCl4})^2$ / J cm^{-3} (Hildebrand estimate)	$\Delta_{vap}h$ [$SiCl_4$] / kJ mol^{-1} (extrapolated)	δ_{SnCl4}/J$^{1/2}$cm$^{-3/2}$	δ_{SnI4}/J$^{1/2}$ cm$^{-3/2}$
0	111.5	148.3	59.4	31.1	16.1	23.8
25.0	115.4	151.1	58.5	29.7	15.4	23.0
40.0	117.2	153.0	57.7	28.9	15.0	22.6
81.3	127.4	157.6	55.5	26.6	13.6	21.1
88.0	129.4	158.8	54.9	26.2	13.4	20.8
112.1	137.2	161.6	52.7	24.9	12.6	19.8
115.6	138.6	162.0	52.3	24.7	12.5	19.7
131.0	145.0	163.7	50.9	23.9	11.9	19.0
132.0	145.4	163.8	46.9	23.8	11.9	18.7
136.0	147.2	164.2	46.2	23.6	11.7	18.5
139.9	149.0	164.7	44.1	23.4	11.6	18.2

List of Figures

Fig. 1 Plot of conservative interaction parameters against temperature derived using our new parameterization method, based on Regular Solution Theory, for the system $SnI_4/SiCl_4$.

Fig. 2 Local density histograms constructed from the final configuration of each DPD simulation. (a) 0 ˚C; (b) 25 ˚C; (c) 88 ˚C; (d) 131 ˚C; (e) 140 ˚C.

Fig. 3 Local coordination number histograms (of $SiCl_4$ species) at different temperatures.

Fig. 4 Temperature-composition diagram for the $SnI_4/SiCl_4$ binary system. Crosses are Thermo-Calc data, obtained using free energy versus temperature data calculated using Eq. (26) with the heat of mixing data taken from Ref. [9]. Filled circles are the data obtained from the DPD simulations after the configurations have been analysed using the local histogram method. Unfilled squares represent actual experimental data as reported by Hildebrand and Negishi [9].

Fig. 5 Local density histograms calculated using $\bar{a}_{11} = \bar{a}_{22} = \bar{a} = 25$, $\bar{\rho} = 3$, at different temperatures. Note that the histogram has not been corrected to remove interfacial contributions, since no phases, and hence no interface, was discernable in these simulations.

Fig. 1: Travis et al

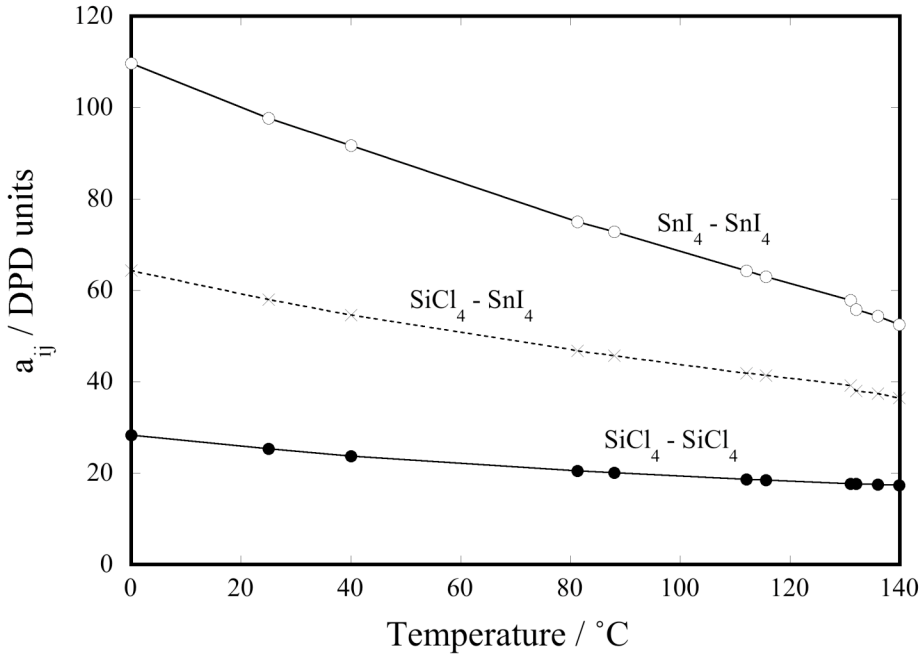

Fig. 2a Travis et al

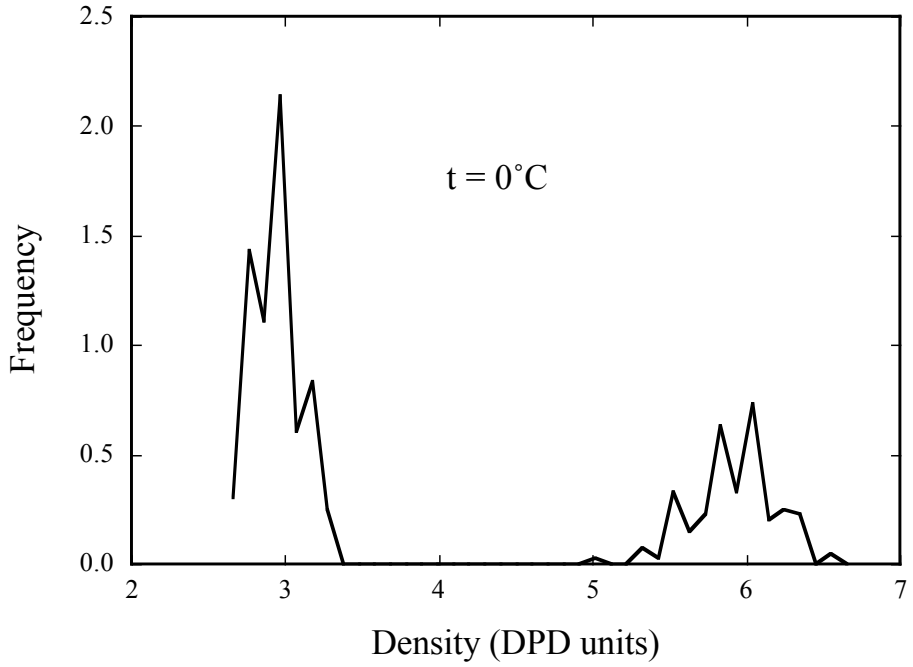

Fig. 2b Travis et al

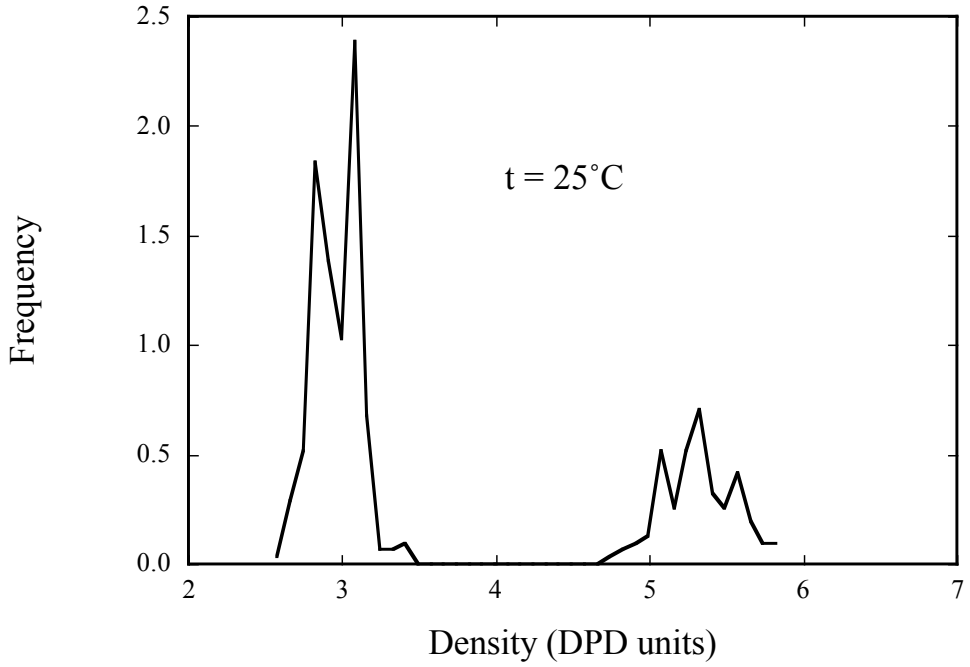

Fig. 2c Travis et al

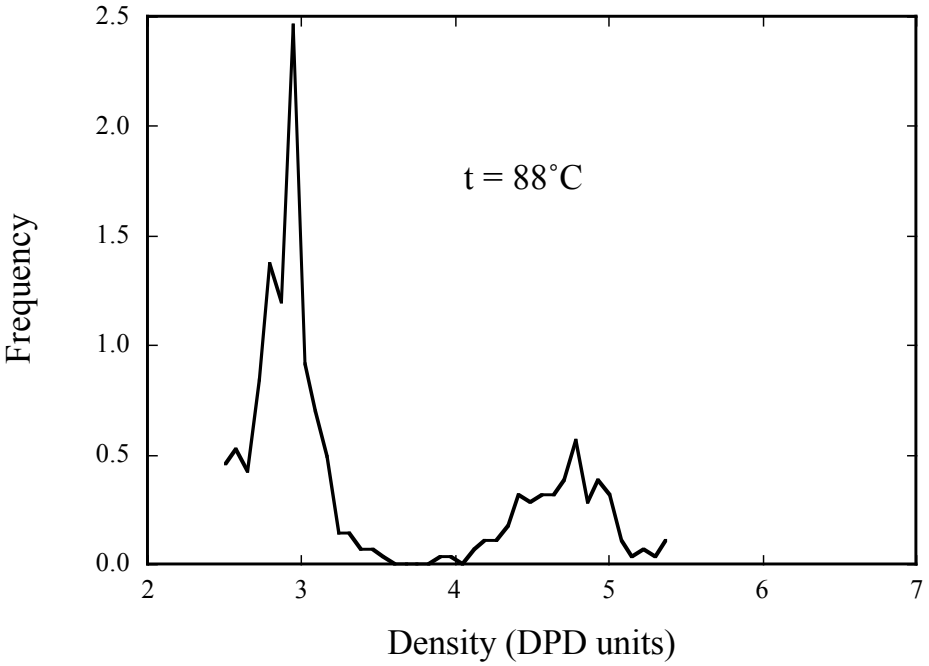

Fig. 2d Travis et al

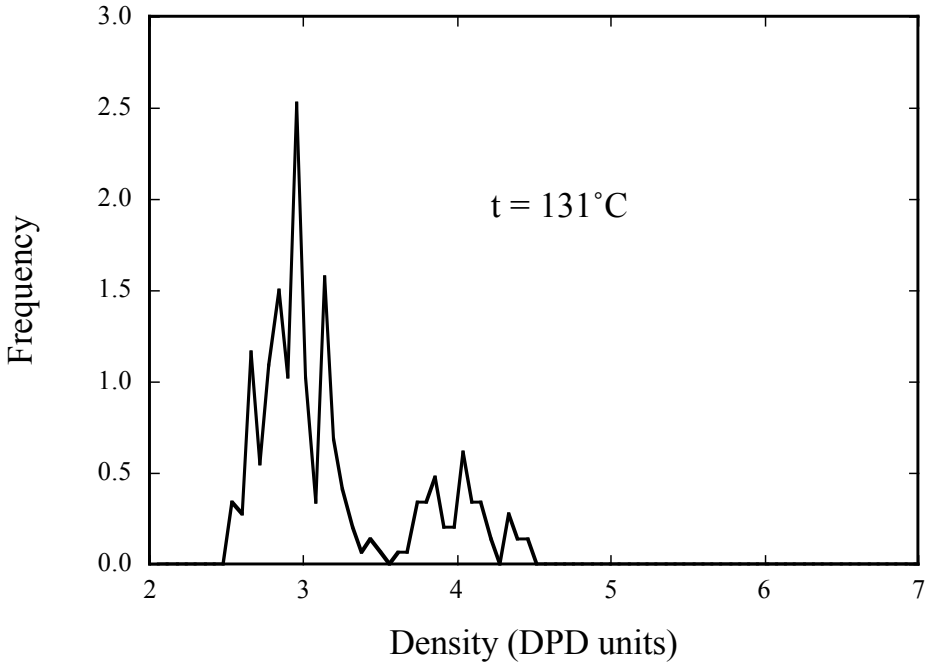

Fig. 2e Travis et al

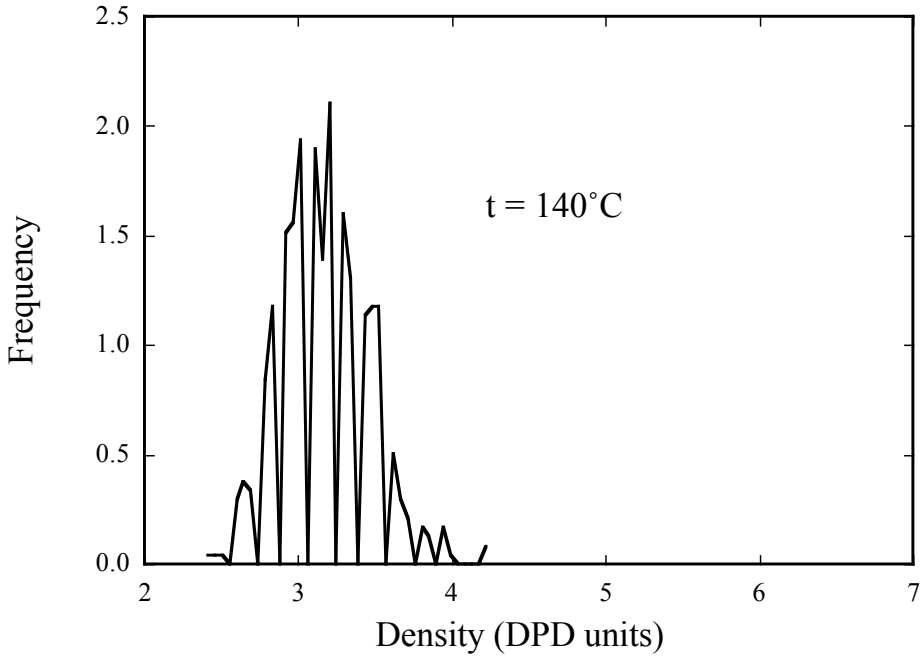

Fig. 3: Travis et al

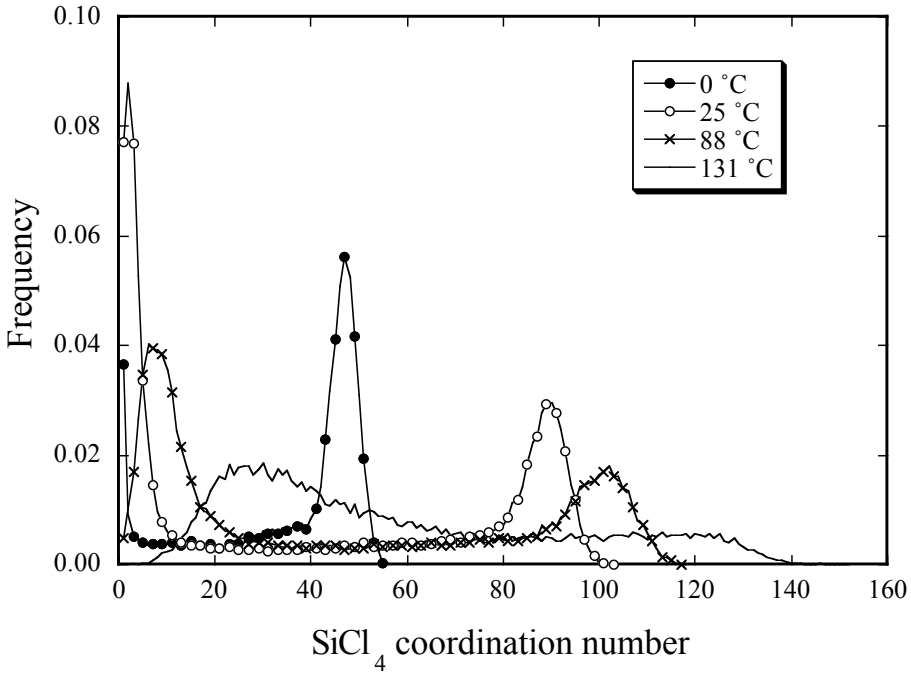

Fig. 4: Travis et al

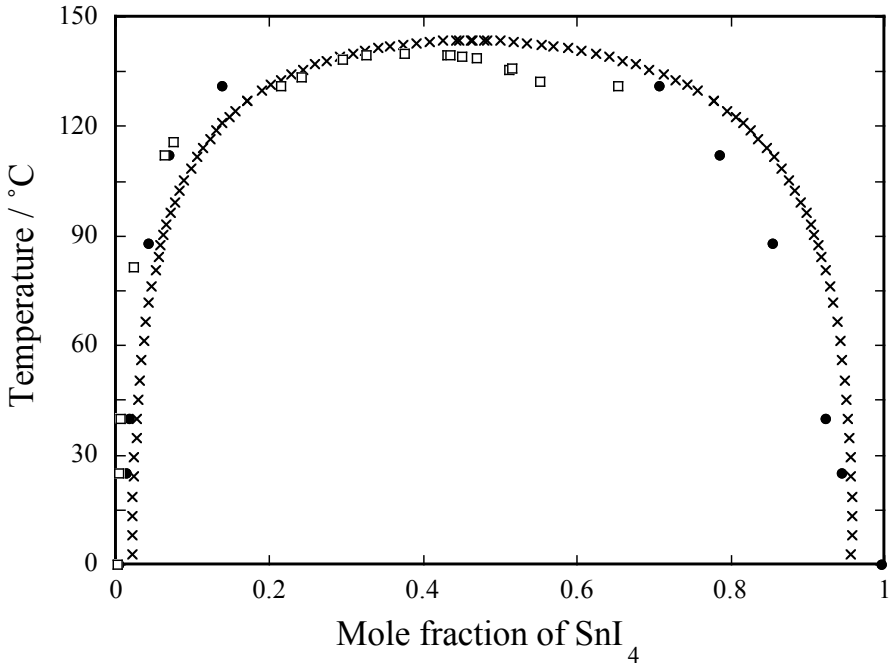

Fig. 5: Travis et al